The Mass-Spring Model as an Alternative to the Finite Element Method in the Heart Valve Movement Simulation

CES Seminar Paper

Sönke Thies

Supervisor: M.Sc. Michael Neidlin
May 2016

Contents

1 Motivation

Heart valve repair is an important task in cardiac surgery. In an aging society the number of heart valve surgeries keeps increasing yet there is little usage of computational medicine tools. A reason is the difficulty to precisely capture the valves geometry, which varies significantly between patients. Another problem is the computation time needed to conduct industry standard Finite Element Method studies. Possble applications would be in surgical planning or even real time simulation during surgery, where low computation time is a key requirement. Hence further research for alternative models is undertaken. A possible model is the mass-spring model, which is also used in computer graphics.

2 Mass-Spring Model

In a mass-spring model a geometry is discretized by elements consisting of nodes and edges connecting the nodes. The mass is completely distributed to its nodes. The edges represent springs with an elasticity variable k as well as dampers with a damping variable d. All acting forces are exerted onto the point masses.

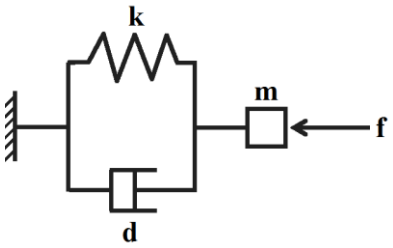

Fig. 1 Scheme of a mass-spring-damper system

2.1 Basic equations

The dynamics of a point mass i are described by Newton's law of motion. The force term f_i is unknown and needs to be modeled.

$$f_i = m_i \ddot{x}_i$$

From Fig. 1 we can see that three types of forces are loaded onto a node. An external force f^{ext}, which is given and doesn't need to be modeled and the internal forces f^d and f^k. The spring force f^k is expressed by Hooke's law and is only valid up to a specific Δx_{max} as it is a linear approximation to the real response of a spring. Δx is the elongation from the springs' rest length. The spring parameter k_{ij} is the stiffness of the spring connecting nodes i and j. It has the unit $\frac{kg}{s^2}$.

$$f_i^k = k_{ij} \Delta x_i$$

The damping force f^d acts against the current direction of motion. It can be interpreted as energy dissipation due to inner friction. The unit of d_{ij} is $\frac{kg}{s}$.

$$f_i^d = d_{ij}\dot{x}_\iota$$

All terms combined lead to the second order differential equation

$$m_i\ddot{x}_\iota = f_i^{ext} - d_{ij}\dot{x}_\iota - k_{ij}\Delta x_i.$$

Summed over all nodes of a mesh and transformed to a first oder differential equation system we get the state-space representation of the model

$$\begin{pmatrix}\dot{\vec{x}}\\ \dot{\vec{y}}\end{pmatrix} = \begin{pmatrix}\vec{y}\\ M^{-1}(\vec{f}^{ext} - D\vec{y} - K\vec{x})\end{pmatrix}$$

with the diagonal matrix of inverted masses M^{-1}. In Cartesian coordinates a mesh with N nodes has vectors of size $\mathbb{R}^{3N}$ and the matrices are of size $\mathbb{R}^{3N\times 3N}$ correspondingly. The total state-space vector is hence of size $\mathbb{R}^{2*3N}$.

2.2 Stiffness matrix comparison of triangular elements

The leaflets of a heart valve are very thin. Models describing the motion of a heart valve are therefore discretized by membrane elements. In paper [1] A. van Gelder examined the stiffness matrices of the constant strain triangle (CST) model from FEM in comparison with a triangular spring mesh model. The constant strain and stress functions of the CST ensure that a loaded triangle remains a triangle. The general stiffness matrix of both models with nodes p, q, r and edges $(p, q), (p, r), (q, r)$ has the form

$$\boldsymbol{K_e} = \begin{bmatrix} K_{pp} & K_{pq} & K_{pr} \\ K_{qp} & K_{qq} & K_{qr} \\ K_{rp} & K_{rq} & K_{rr} \end{bmatrix}.$$

Consider two-dimensional nodes in an x-y-frame and let e.g. x_{ij} be an abbreviation for the distance $x_i - x_j$, where x_i is the x-position of node i. Let further be $E_2 = Et$ the "two-dimensional Young's modulus". The variable t represents the thickness of the membrane. In the two-dimensional case the submatrices of $\boldsymbol{K_e}$ are 2×2 matrices. Given the Poisson ratio ν the diagonal elements of the CST model have the form

$$K_{pp}^M = \frac{E_2}{4area(T_e)(1-\nu^2)}\begin{bmatrix} y_{rq}^2 + \frac{(1-\nu)}{2}x_{rq}^2 & -\frac{(1+\nu)}{2}y_{rq}^2\, x_{rq}^2 \\ -\frac{(1+\nu)}{2}y_{rq}^2\, x_{rq}^2 & x_{rq}^2 + \frac{(1-\nu)}{2}y_{rq}^2 \end{bmatrix}$$

and the off-diagonal entries are

$$K_{pq}^M = \frac{E_2}{4area(T_e)(1-\nu^2)}\begin{bmatrix} y_{rq}y_{pr} + \frac{(1-\nu)}{2}x_{rq}x_{pr} & -\nu y_{rq}x_{pr} + \frac{(1-\nu)}{2}y_{pr}x_{rq} \\ -\nu x_{rq}y_{pr} - \frac{(1-\nu)}{2}x_{pr}y_{rq} & x_{rq}x_{pr} + \frac{(1-\nu)}{2}y_{rq}y_{pr} \end{bmatrix}.$$

All other elements can be obtained by permuting p, q and r accordingly.

For comparison with the mass-spring model we still need its stiffness matrices. The rest length of spring (i, j) is L_{ij}. Like in section 2.1 the spring stiffness parameter is k_{ij}. For a model, where the nodes may rotate freely and the elongation or compression of a spring causes a one-dimensional stress we get the submatrices

$$K_{pp}^S = E_1 \begin{bmatrix} \frac{k_{qp}x_{qp}^2}{L_{qp}^3} + \frac{k_{pr}x_{pr}^2}{L_{pr}^3} & \frac{k_{qp}x_{qp}y_{qp}}{L_{qp}^3} + \frac{k_{pr}x_{pr}y_{pr}}{L_{pr}^3} \\ \frac{k_{qp}x_{qp}y_{qp}}{L_{qp}^3} + \frac{k_{pr}x_{pr}y_{pr}}{L_{pr}^3} & \frac{k_{qp}y_{qp}^2}{L_{qp}^3} + \frac{k_{pr}y_{pr}^2}{L_{pr}^3} \end{bmatrix}$$

on the diagonal of $\boldsymbol{K_e}$. The off-diagonal elements have the form

$$K_{pq}^S = E_1 \begin{bmatrix} -\frac{k_{qp}x_{qp}^2}{L_{qp}^3} & -\frac{k_{qp}x_{qp}y_{qp}}{L_{qp}^3} \\ -\frac{k_{qp}x_{qp}y_{qp}}{L_{qp}^3} & -\frac{k_{qp}y_{qp}^2}{L_{qp}^3} \end{bmatrix}$$

and as before all other elements can be obtained by cyclic permutation of p, q and r.

The goal is to equal the spring model to the CST model. The only unknown variable is the spring stiffness parameter k_{ij}. Hence an expression for k_{ij} is needed. Consider e.g. the attempt to equal the upper right off-diagonal entries of both models

$$\left(K_{pq}^S\right)_{12} = \left(K_{pq}^M\right)_{12}.$$

There exists no general choice of k_{pq} to equal these entries. If x_{qp} or y_{qp} are zero one could not solve for k_{pq}. The same holds for other entries. It is therefore in general not possible to equal both models.

The element matrices are singular and thus have no unique solution, which could be an option that different stiffness matrices share the same equilibria. However, van Gelder showed in his paper, that no physically realistic value $\nu \leq 0.5$ exists such that the mass-spring model could exactly simulate the CST model.

Any solution of the mass-spring-model can thus be only an approximation to the CST model.

2.3 Model parameters

As discussed earlier we try to find the stiffness and damping parameters that best approximate a constant strain model.

2.3.1 Stiffness parameter

Not only did van Gelder show in his paper [1], that an exact solution is not possible he also derived an approximation of the stiffness parameter in it. It is restricted to simulate an isotropic elastic membrane to the first order of linear deformations. The derivation consists mainly of geometrical aspects. For a single triangle it leads to the equation

$$k_c = \left(\frac{E_2}{1+\nu}\right)\frac{area(T_e)}{|c|^2} + \left(\frac{E_2\nu}{1-\nu^2}\right)\frac{(|a|^2+|b|^2-|c|^2)}{8area(T_e)}$$

given a triangle with edges a, b and c. The parameter k_c denotes the spring stiffness of edge c. Once again the other parameters can be obtained by correct permutation. One way to compute the area of a triangle is by using the equation

$$area(T_e) = \frac{1}{4}\sqrt{(|a|+|b|+|c|)(|a|+|b|-|c|)(|a|-|b|+|c|)(-|a|+|b|+|c|)}$$

For an obtuse triangle the term $|a|^2+|b|^2-|c|^2$ becomes negative and since $\nu \geq 0$ the stiffness parameter could also be zero or negative. If this is physically reasonable is highly questionable. To avoid obtuse triangles in a mesh an adaptive remeshing procedure during the solve routine could be an option. Depending on implementation, mesh and load an "on-the-fly"-remeshing routine could highly increase the computational cost, which contradicts the goal to simulate the motion of the heart valve as fast as possible. Van Gelder suggested to restrict his formula thus to the case $\nu = 0$. Additionally, it needs to be considered, that an edge is part of two triangles if it is not a boundary edge and therefore the adjacent areas are summed. Finally, above's equation transforms to

$$k_c = \frac{E_2 \sum_e area(T_e)}{|c^2|}$$

He found that making all k in a mesh equal leads to distortions at equilibrium even for small deformations in a uniform loaded test case. They disappeared with assigning above's stiffnesses to the springs.

In 2007 Lloyd and his team did more research [2] on the spring parameter and without giving the exact derivation, but noting that for $\nu = 1/3$ the triangle must be equilateral the spring parameter can be expressed as

$$k = \sum_e Et\frac{\sqrt{3}}{4}$$

Now this would mean that all non-boundary stiffnesses are equal and all boundary values are half the non-boundary value. There is also no state-dependency anymore. By maximum error comparison with FEM simulations it was found that $\nu = 1/3$ yields the least error, which agrees with Llyod's theory. van Gelder's equation and Lloyd's equation become equal for equilateral triangles. As a consequence, they noted that his formula is not valid for $\nu = 0$, but for $\nu = 1/3$. Admitting that, taking the areas into account and hence making the parameters non-equal is advantageous they finally suggested to use van Gelder's equation, which rewritten transforms to

$$k_{ij} = \sum_e Et\frac{\sqrt{3}}{4}\frac{A_e}{A_0}$$

A_0 is the area of an equilateral triangle with length l_{ij}.

2.3.2 Damping parameter

The damping parameter represents the energy dissipation in the model. It may occur as a result of different physical effects. External effects such as interaction of the valve with a surrounding fluid shall not be considered here. The internal energy dissipation can be interpreted as imperfect elasticity due to inner friction. An undamped model would oscillate around its equilibrium position once a force has been applied. At least on the scale of accuracy considered here ($\sim 1e^{-5}m$) this would be unphysical. Hence we know that d has to be positive, slowing down the total system. Not only has physical correctness to be taken into account, but also numerical stability.

In paper [3] Bhasin and Liu described bounds of stability for the explicit Euler scheme. The example is examined for a node attached to a fixed boundary. The lower bound is derived from the observation that an underdamped system $d_{ij}^2 - 4m_i k_{ij} < 0$ oscillates. As oscillations shall not occur they follow that $d_{ij} \geq 2\sqrt{k_{ij} m_i}$. The upper bound is derived from the reasoning that the change in velocity during a timestep may at most cause a node to stop. Damping forces may thus not be dominant with respect to the change in velocity due to stiffness. Combined it results that

$$2\sqrt{k_{ij} m_i} \leq d_{ij} \leq \frac{|v_i^t \frac{m_i}{\Delta t} + f_i^{k|t}|}{|v_i^t|}, \qquad |v_i^t| \neq 0$$

should hold. $f_i^{k|t}$ is the spring force at time t.

There occurs a problem with different mesh resolutions if $d_{ij} = 2\sqrt{k_{ij}(m_i + m_j)}$. As shown in paper [5] applied to a volumetric mesh, but analogously applicable to a surface mesh, different mesh resolutions lead to significant variations in node positions. This is why they scaled the damping to the length l of a spring, resulting in $d_{ij} = \frac{2\sqrt{k_{ij}(m_i+m_j)}}{l_0}$. This minimizes the influence of mesh resolutions. Note that the damping coefficient becomes significantly larger than the lower bound (critically damped case) for small l.

Up to the current day there exists no derivation for the damping coefficients from physical theories such as viscosity. This is a main drawback, when using mass-spring systems. While algorithm stability and speed is necessary the combination of stiffness and damping parameters to correctly simulate a motion is often a process of trial and error. There may not even exist such a pair to reach physical correctness without losing the main goal of computational speed. Also one has to consider that finding an appropriate set of parameters for different geometries also takes time.

2.4 Material parameters

While the model parameter selection is a challenge, the material parameters and the geometry for different heart valves also vary significantly. The thickness of a mitral valve has for example been described from 0.7 mm [6] on average for porcine mitral valve leaflets up to 1 mm in a

simulation [7]. In paper [8] it was described that different regions of a mitral valve have different thicknesses ($0.2 - 1.2$ mm).

2.4.1 Young's modulus

Young's moduli for heart valves have been examined in paper [6] and [8]. In [6] tensile tests of porcine mitral valves, which are believed to be similar to human mitral valves, were executed. In paper [8] prestrain and in-vivo versus in-vitro effects were reported.

Heart valve tissue behaves anisotropically. Biaxial tests on excised pork valves showed a difference in circular and radial directions [6]. In figure 2 the circles denote the circumferencial and the triangles the radial direction. The anterior and posterior leaflets are the two leaflets of the mitral valve. At different strain rates both leaflets exihibit a steep increase in stress. There was also a slight hysteresis effect reported.

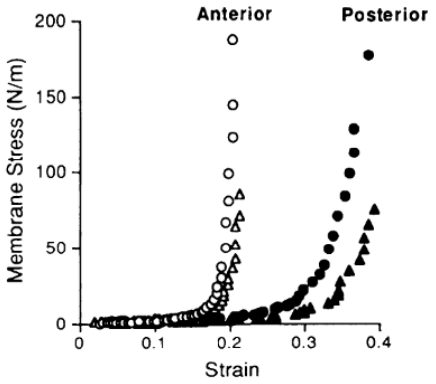

Fig. 2 Mechanical behavior of porcine mitral valve leaflets [6]

Indications in paper [8] show that the leaflets are prestrained and reach the area of non-linearity during the deformation phase.

To account for the non-linearity a simple model that described the Young's modulus as an exponentital function was formed [9]. Young's modulus can be expressed as the ratio of stress and strain $E = \frac{\sigma}{\varepsilon}$. λ and κ are two unique parameters such that the exponentital function fits the stress-strain behavior. Replacing Young's modulus in the spring stiffness equation leads to

$$k_{ij} = \frac{\lambda e^{\kappa\varepsilon} \sum A_e}{\varepsilon l_{ij}}$$

2.4.2 Poisson coefficient

Because of the high water content soft tissue is usually described to have a poisson coeffient close to 0.5. There exists no precise data from experiments for heart valves. In section 2.3.1 numerical experiments showed that the derived equation gives the least error for $\nu = 0.33$. One could try another value using the more complicated equation for k_{ij} if a mesh procedure is used that does not allow obtuse triangles.

2.5 Force direction

The force of a spring can not be simply expressed by $k\vec{x}$ as it only acts along the direction of it. The force f_i^k between two points x_i and $x_j$is thus corrected by the unit vector in the direction of the spring and the elongation from its rest position.

$$x_i = (x_i, y_i, z_i)^T$$

$$f_i^k = k_{ij}(l_{ij} - l_{ij}^0)\frac{x_i - x_j}{l_{ij}}$$

In matrix notation it is expressed as $\hat{K}\vec{x}$. Now the question arises whether the damping forces have to be treated in a similar way. By defining the damping forces as $D\vec{y}$ all velocities including rotational velocities of a node attached to a non-elongated spring would be damped. The main problem that arises is that there exists no theory for damping, see section 2.3.2. It is questionable whether rotational velocities should not be damped at all or by some value that might be connected to internal friction. In several cases, where mass-spring models are used [4] the damping forces are corrected by the square of its directional unit vector. This makes the damping not only state-dependent on $\vec{v}$, but also on the position due to componentwise multiplication.

$$f_i^d = d_{ij}\frac{(x_i - x_j)(x_i - x_j)}{l_{ij}}\frac{v_i - v_j}{l_{ij}}$$

Similarly to the stiffness equation, the matrix notation is then $\hat{D}\vec{v}$.

3 Simulation Results

I implemented a model in MATLAB that uses van Gedler's equation for the springs. The differential equations of a mass-spring system are stiff. Therefore, the solver used for the first order state-space system is MATLAB's inbuilt ode15s method.

The material parameters are:

Thickness of the leaflet (t)	0,0006 m
Young's modulus (E)	60000 Pa
Poisson ratio (v)	0,333333
Density (ρ)	1060 $\frac{kg}{m^3}$

The test geometry is a semi-circle with a coarse mesh consisting of 52 nodes and 73 triangles, see figure 3. The semi-circle is fixed, 21 of the 52 nodes are boundary nodes. The diameter is $0.02m$.

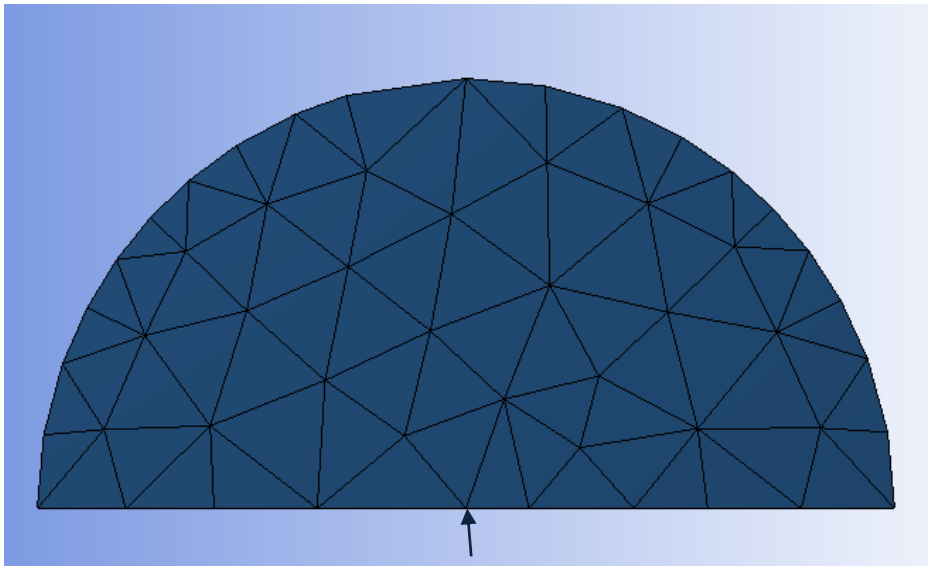

Fig. 3 Semi-circular coarse test mesh

The geometry is loaded with the pressure function $p = 944t$ Pa for half a second. The pressure at $t = 0.5s$ corresponds to the maximum pressure exhibited on a mitral valve during the filling process of the left ventricle. A basic test comparison is done with the program ANSYS Transient Structural. There is no damping in the FEM simulation. The relative error tolerance is 0.001, the absolute error tolerance is $0.01mm$. Both models use adaptive time stepping with a maximum timestep of $0.001s$. The damping coefficient in the mass-spring model is alternated between 3 cases and rotations are also damped.

Case 1: $d_{jj} = 2\sqrt{k_{ij}(m_i + m_j)}$, which is equal to critical damping

Case 2: $d_{jj} = \frac{2}{l_0}\sqrt{k_{ij}(m_i + m_j)}$, mesh independent damping

Case 3: $d_{jj} = \frac{2s}{l_0}\sqrt{k_{ij}(m_i + m_j)}, s = const = 0.04$, mesh independent corrected damping

In figure 4 and 5 the z- and x-position of the "peak" node, which is marked by an arrow in figure 3, are plotted. The y-position change is neglectable. The oscillations in the FEM case occur, because no damping is applied. For case 1 both positions overshoot the predicted position by the FEM solver. Especially the difference in the x-position significant. In case 2 the damping is so high, because of the low l_0, that almost no motion in the mass-spring model occurs. The corrected case 3 also shows a significant difference from the FEM model. It might still be advantageous to use equation referred to l_0, because the computation time in these cases has been significantly lower. However, the difference in positions is too large for the model to be applied in reality.

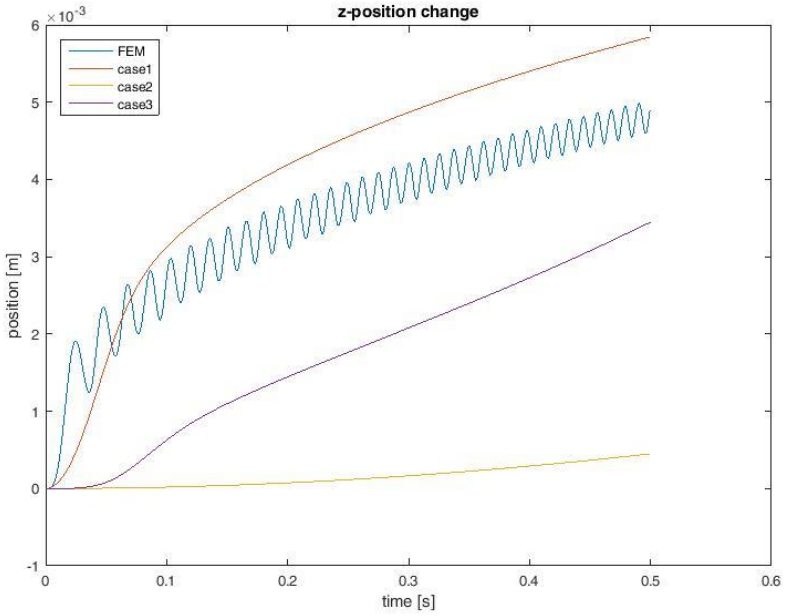

Fig. 4 z-position of the “peak” node

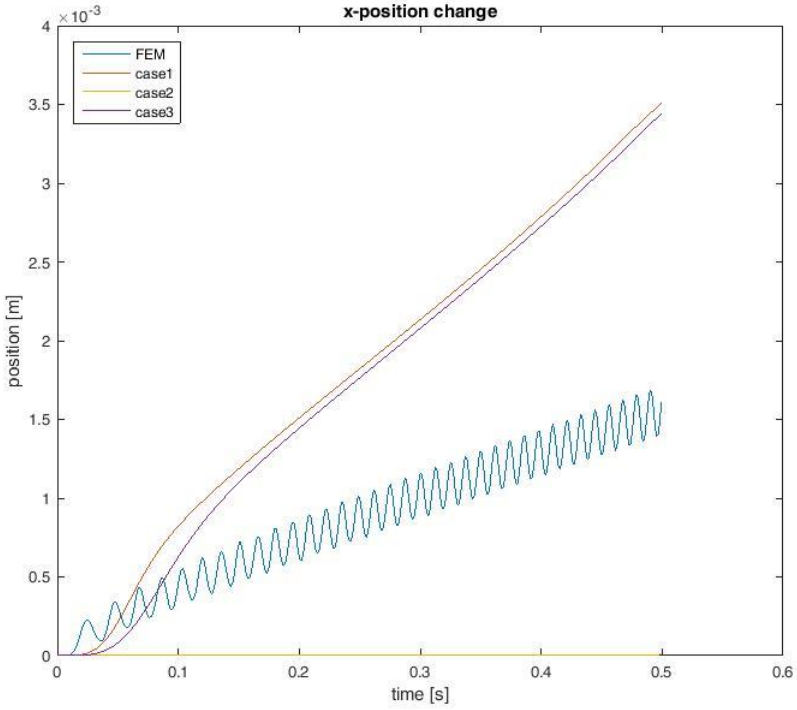

Fig. 5 x-position of the “peak” node

4 Discussion

Heart valve mass-spring models so far in literature [7], [10], [11] share in common, that they only assess static loading, although implemented as dynamic models. This is most likely due to the inability to precisely simulate the motion, because of the mentioned problem in section 2.3.2 of finding the right damping parameters. As shown in section 2.3.1 there exist theories how to assign the spring stiffnesses with van Gelder's approach still being the most popular. It is however simplified, because it does not take the anisotropy of a real material into account. There exist models that simulate anisotropy, e.g. [11], but there is no derivation of any equations given. The chosen model parameters are fitted by trial and error such that the behavior in sense of accuracy and computational speed is optimal for a specific case. The current application of a mass-spring model can thus at most be to answer basic questions, if e.g. a leaflet will close under a given peak pressure or not. Implementing a more sophisticated mass-spring model is often not desired as it would take away the execution time advantage compared to a FEM simulation. The validation of mass-spring as well as FEM models is troublesome, because of the varying geometries and material parameters. Assisting a surgeon in real time with a relatively precise model is hence not possible.

References

[1] A. Van Gelder. Approximate Simulation of Elastic Membranes by Triangulated Spring Meshes. 2004

[2] B. A. Llyod, G. Székely, M. Harders. Identification of Spring Parameters for Deformable Object Simulation. 2007

[3] Y. Bhasin, A. Liu. Bounds for Damping that Guarantee Stability in Mass-Spring Systems. 2006

[4] Y. Duan, W. Huang et. al. Volume Preserved Mass-Spring Model with Novel Constraints for Soft Tissue Deformation. 2016

[5] C. Paloc, F. Bello et. al. Online Multiresolution Volumetric Mass Spring Model Real Time Soft Tissue Deformation. 2002

[6] K. May-Newman, F. Yin, Biaxial mechanical behavior of excised porcine mitral valve leaflets. 1995

[7] P. Hammer, D. Perrin et. al., Image-based mass-spring model of mitral valve closure for surgical planning. 2008

[8] M. Rausch, N. Famaey et. al., Mechanics of the mitral valve. 2013

[9] W. Gao, L. Chu et. al., A Non-Linear, Anisotropic Mass Spring Model based Simulation for Soft Tissue Deformation. 2014

[10] N. Tenenholtz, P. Hammer et. al., On the Design of an Interactive, Patient-Specific Surgical Simulator for Mitral Valve Repair. 2011

[11] P. Hammer, P.J. del Nido et. al., Anisotropic Mass-Spring Method Accurately Simulates Mitral Valve Closure from Image-Based Models. 2011